Article

Supercapacitors of Nanocrystalline Covalent Organic Frameworks—A Review

Jingjie Xia [1,2,†], Ronghao Wang [1,2,†], Chengfei Qian [1,2,†], Kaiwen Sun [3], He Liu [1,2], Cong Guo [1,2], Jingfa Li [1,2], Feng Yu [1,2] and Weizhai Bao [1,2,*]

1 Institute of Advanced Materials and Flexible Electronics (IAMFE), School of Chemistry and Materials Science, Nanjing University of Information Science and Technology, Nanjing 210044, China
2 Department of Materials Physics, School of Chemistry and Materials Science, Nanjing University of Information Science and Technology, Nanjing 210044, China
3 Australian Centre for Advanced Photovoltaics, School of Photovoltaic and Renewable Energy Engineering, University of New South Wales, Sydney 2052, Australia
* Correspondence: weizhai.bao@nuist.edu.cn
† These authors contributed equally to this work.

Abstract: Due to their highly changeable porosity and adaptable skeletons, covalent organic frameworks (COFs) have been frequently used in supercapacitors. Additionally, COFs are a wonderful match for supercapacitors' requirements for quick carrier migration and ion catalysis. COFs exhibit significant potential and limitless opportunities in electrochemical storage supercapacitors. The applicability of COFs has, nonetheless, been limited because the primary organic component prevents electron conduction and the interior active sites are challenging to fully utilize. The conductivity enhancement of COFs has been the subject of extensive research to solve these challenges. This review begins by outlining the features of COFs in the context of their use in supercapacitors and their methods of synthesis. The application of previously published COF materials in supercapacitors were evaluated including electrode materials and solid-state devices. Finally, essential aspects and potential problems are discussed as the exceptional performance characteristics of COFs are illustrated from a supercapacitor standpoint. This review also forecasts the future of COF-based supercapacitor development.

1. Introduction

Quick consumption of fossil fuels, and progressive depletion of natural resources have resulted in a slew of environmental issues [1]. Countries all over the world are working hard to produce and use clean energy to maintain the ecological environment and the long-term growth of the global economy. Renewable energy sources are, nevertheless, significantly influenced by climate, topography, and a variety of other factors. The advancement of energy storage and conversion devices, such as batteries and supercapacitors, is critical [2–6]. Many scientific studies have been drawn to supercapacitors because of their high-power densities, fast charging and discharging rates, long performance lives, and wide range of operating temperatures [7,8]. Supercapacitors have apparent advantages in power density over batteries, which has encouraged the development of supercapacitors worldwide.

The electrode materials of supercapacitors should match the following criteria for higher capacitance storage and better cycle stability: (1) large specific surface area, (2) high conductivity, (3) acceptable porosity, and (4) stable structure. Supercapacitors should have high capacitance, power density, and energy density, as well as fast charging and discharging and great cycle stability. Traditional double-layer supercapacitors store energy through generating a double electric layer within the interface of electrode and the liquid electrolyte. The traditional matrix material for electrochemical double-layer supercapacitors (EDLCs) is

primarily from the carbon-based family with a high specific surface area. Activated carbon (AC), with its high conductivity, large specific surface area, relatively stable structure, and wide choice of raw materials, remains the primary electrode material for commercial EDLCs. [3] Another important type of supercapacitor, depending on the energy storage principle, is faradaic supercapacitors (FSs) or pseudo-capacitors. Since pseudo-capacitors store energy through quick and reversible redox processes on the electrode surface, their energy density is at least one order of magnitude greater than that of EDLCs. Pseudo-capacitor electrode materials, on the other hand, have specific requirements for porosity, pore size and distribution, and redox groups. As a result, researchers have focused on a type of porous organic polymer, known as the covalent organic framework. However, this research hotspot has few review reports.

Covalent organic framework materials are crystalline organic porous materials made up of building motifs connected by an organized network of covalent connections. COFs have been widely used in sorption, catalysis, optoelectronics, separation, storage, and other fields, since Professor Yaghi and his colleagues first synthesized the two-dimensional materials, COF-1 and COF-5, in 2005, as kinds of crystalline porous organic polymers (PoPs) with a permanent porous structure and an altitudinal ordered structure. COFs are also prominent in the disciplines of electrochemical energy storage (EES) and electrochemical energy conversion (EEC) because of their unique structural properties. Much research discovered COFs are appropriate materials for electrodes when Dichtel et al. successfully applied COF to supercapacitors in 2015. COF has the following characteristics that fully match the electrode material requirements of supercapacitors: (1) high specific surface area and stable structure, (2) high porosity, (3) channel suitable for charge transmission, and (4) well-defined structures and functional skeletons. There have been few reviews on this topic, so it is necessary to review representative COF-based supercapacitors. (Figure 1).
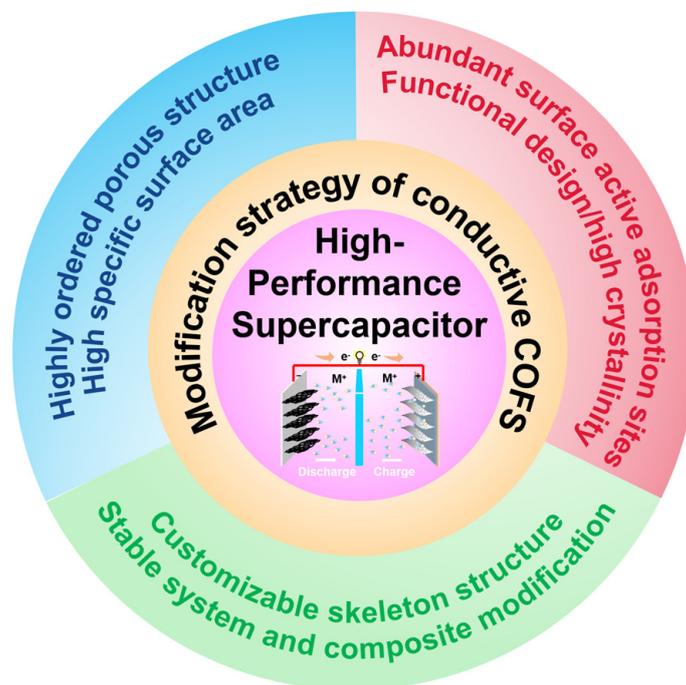
Figure 1. Schematic diagram of modification strategy of conductive COFS in supercapacitors.

Herein, this review begins by defining the characteristics of COFs in the context of their employment in supercapacitors, as well as their production methods. Following that, the usage of previously described COF materials in supercapacitors is examined in terms of electrode materials and solid-state devices. Finally, as the extraordinary performance characteristics of COFs are presented from a supercapacitor standpoint, crucial aspects

and potential issues are explored. This review also projects the future development of COF-based supercapacitors.

2. Characteristics of COF Materials for Supercapacitors

Covalent organic frameworks (COFs), occupy adjustable and periodic pores [9,10], have relatively high porosity [11–14] and clear structures [15,16], and a multi-functional framework [17]. COFs, according to the geometric symmetry of the crystal, can be simply divided into two types: two dimensional-based COFs and three dimensional-based COFs. Yi Meng and co-workers found that the design of functional groups could influence the dimensionality of COFs, as well as their functionality. They concluded that functional moieties integration allows the resulting COF materials to have different properties [18]. As for supercapacitors, two dimensional-based COFs, such as COF nanosheets, can help the electrolyte to wet the electrode surface and absorb ions, thereby improving its specific capacitance [19]. On the one hand, COFs have an inherently large surface area, which provides a wealth of adsorption sites, and, on the other hand, the π-electronic skeleton-based COFs, with highly ordered porous architectures, offer the ideal ion transport path in the electrode–electrolyte interface [20]. These characteristics are beneficial to ameliorate the performance of electrochemical double-layer capacitors (EDLCs) and pseudo-capacitors.

After a large number of scientific studies, research found that the nanostructure of COFs is one of the most crucial reasons for its application in supercapacitors. There is no doubt that the extremely high surface area and high crystallinity make COFs one of the rare energy storage materials in the world that can be used in supercapacitors. As mentioned above, the large number of adsorption sites is due to the desirable high surface area and porosity of COFs, which is one of the reasons why researchers have applied them to energy storage in recent years. For example, the following COFs have achieved a high level of BET surface area: Phos-COF-1 (818 m^2/g), PT-COF (1998 m^2/g), and TpOMe-DAQ (1531 m^2/g). Meanwhile, the high crystallinity determines the outstanding stability of the COF material and its ability to continue to be used after many charging and discharging cycles. Remarkably, the energy storage mechanisms of many COF materials are still unknown. However, it is certain that its clear nanostructure will help further future research on its energy storage mechanism and facilitate the development of better performance COF-based supercapacitors. Therefore, in our opinion, the study of COFs' nanostructure is vital for COFs to be used for better energy storage.

3. Synthesis Strategies of COFs for Supercapacitors

In the next section, we briefly introduce several commonly used synthesis strategies, which are divided into a top-down and bottom-up strategy [21–23].

3.1. Bottom-Up Strategy

This is an important approach for growing COF nanosheets and thin films on specific substrates or interfaces. The key lies in the preorganization of the precursor to control the growth direction of the film and avoid disorderly extension of the film. In this section, we focus on the solvothermal method, which is the most frequently utilized method.

Solvothermal Method

The solvothermal approach is a mature COF synthesis process. Solvothermal synthesis is a type of wet-chemical synthesis that involves immersing an appropriate substrate in a covalent organic framework reaction mixture, followed by washing and drying procedures to increase purity. The high-pressure solvent method can increase reaction rate and improve crystallinity. For example, a conventional synthesis process of COF-5 involves polymerizing HTTP-1 with PBBA-5 using the high-pressure solvent method [24]. Certainly, there is another way to synthesize COF-5. For instance, Dichtel et al. synthesized an oriented 2D layered COF film on the surface of single-layer graphene (SLG). Directional 2D layered COF films were synthesized on single-layer graphene (SLG) under simple solvothermal

conditions. The layered films, stacked perpendicular to the SLG surface, showed improved crystallinity compared with COF powder [25].

3.2. Top-Down Strategy

Two-dimensional COFs, as we know, are layered structures. The different individual layers are piled vertically by weak contacts, such as hydrogen bonding and/or van der Waals force. COF nanosheets can be fabricated by the top-down synthesis process by disrupting the interactions between COFs in adjacent layers. In this part, we look through top-down approaches for removing COFs from mechanical exfoliation.

Mechanical Delamination

Banerjee et al., synthesized a series of thermally and chemically stable functionalized covalent organic skeletons (COFs), namely TpPa-NO_2, TpPa-F_4, TpBD-$(NO_2)_2$, TpBD Me_2 and TpBD-$(OMe)_2$, through a solvothermal aldehyde amine Schiff base condensation reaction. At the same time, the synthesized COFs were successfully layered through simple, safe and environmentally friendly mechanical grinding, and the shells were converted into covalent organic nanosheets (CONs) [26]. Then, Banerjee et al. synthesized three thermally and chemically stable equireticular covalent organic frameworks (COFs) by solvent-free mechanochemical grinding at room temperature. They had a layered morphology similar to graphene (exfoliated layer) [27]. They fabricated eight chemically stable COFs via the solvothermal aldehyde-amine base condensation reaction. Then, these COFs were placed in a mortar containing 1–2 drops of methanol and ground using a pestle for 30 min at room temperature. Finally, after completely removing the solvent via evaporation, the COF nanosheets were produced. The thickness of the structures ranged from 3 to 10 nm, which corresponded to 10–30 COF layers. The COF nanosheets retained their structural integrity following delamination. Furthermore, these COF nanosheets, like their parent COFs, were stable in aqueous, acidic, and basic solutions.

Differing from the pestle grinding method mentioned above, ball milling [28,29] is a stable and simple mechanical delamination to exfoliate COFs. For example, the synthesis process of COF nanosheets via condensation reaction were fabricated via ball milling in [30]. To begin, COFs were made using the solvothermal process. Second, for 24 h, these COFs were wet-ball milled with dimethylformamide (DMF) at 225 rpm and then sonicated for 30 min. Finally, centrifugation was used to obtain tsupernate-containing COF nanosheet.

4. COF Based Electrochemical Energy Storage Devices

The supercapacitor, as a new form of energy storage device, combines the quick charging and discharging features of regular capacitors and the energy storage qualities of batteries [31,32]. Super capacitors have drawn a lot of attention from researchers over the years due to their high-power density, extended cyclic life, high Coulomb efficiency, fast charge and discharge rate, and green environmental protection. The current challenge for supercapacitors is to continue improving their energy density.

Generally, the maximum π-overlap is considered to be the most efficient mode for charge transport in an orderly packed molecular system [33]. Coincidentally, two-dimensional COFs have high crystallinity and tightly packed aromatic moieties, which makes 2D COFs an ideal platform for charge carrier transport [34]. In 2D COFs, periodically eclipsed π-stacking columns could act as direct channel paths for charge carrier transport [35]. This section outlines previous research on the application of COF materials to supercapacitors from two perspectives: electrode materials and solid-state devices.

4.1. COF-Based Electrode Materials

COF materials are frequently coupled with other conductive materials for usage in supercapacitors because the conductivity of COFs is limited by disordered regions and particle boundaries. In this section, we discuss COF research in recent years on supercapacitors by functional group.

4.1.1. DAAQ-Based COFs Electrode Materials

Two dimensional COFs have boron-containing bonds that are unstable in oxidation and hydrolysis, restricting their use as electrode materials, especially at high potentials. In 2013, Dichtel's team successfully applied COFs to supercapacitors. They synthesized DT-BASED COF by using the redox 2,6-diaminoanthraquinone (DAAQ) as the precursor, and found that this β-ketoenamine-linked 2D COF showed a reversible electrochemical process of its anthraquinone subunit, with good stability against highly acidic electrolytes. The as-prepared electrodes with decorated COF showed a specific capacitance of 48 ± 10 F·g^{-1} at 0.1 A·g^{-1}, and a specific capacitance of 40 ± 9 F·g^{-1} after 10 cycles, and did not observe significant decrease after 5000 cycles. However, due to the randomness of the DT-BASED COF particle orientation in the electrodes, only 2.5% of the DAAQ moieties (redox-active groups) were utilized [36]. Thereafter, in order to solve this problem, this research team successfully synthesized the first DT- COF oriented film on Au substrates in 2015, and 80%~99% of the active group in the COF electrode was electrochemically accessible. Compared with the same COF synthesized as a randomly oriented microcrystalline powder, the capacitance value increased by 4 times and the charge storage capabilities of DT-COF improved from 0.4 to 3 mF cm^{-2} [37]. In 2016, researchers electropolymerized PEDOT within the matrix of DT-COF COF films. It was found that the PEDOT-modified COF films had a synergistic effect, that is, the PEDOT in the pores effectively connected the redox-active groups of the COF to the electrodes. This enabled the use of thicker films and significantly faster charging rates. The COF film could be charged at a speed of 10–1600C without affecting performance, and could still maintain a stable capacitance after 10,000 cycles [38].

Additionally, an anthraquinone-based COF/graphene composite aerogel (D-COF/GA) was applied to supercapacitors as an electrode material in [39], as shown in Figure 2a. Such COFs were fabricated by electrostatic self-assembly of two materials, each of which had a different charge and was attracted by a positive and negative electrode to achieve the effect. The asymmetric supercapacitor assembled from D-COF/GA and GA, exhibited an outstanding electrochemical performance with an energy density of 30.5 W h kg^{-1} at a power density of up to 700 W kg^{-1}. In 2022, DT-COF prepared with high pH value was applied to the anode of a novel aqueous lithium-ion capacitor for the first time, and it showed good electro-chemical performance. At 0.1 A g^{-1} current density, the capacitor had a good energy storage capacity of 224 F g^{-1}, supercapacitor-level power density of ~4000 W kg^{-1}, and excellent cyclability in 1000 cycles. Moreover, it had excellent lithium ion storage capacity of 108 mAh g^{-1} at 10 A g^{-1} (87% of theoretical specific capacity) and discharge specific capacity of 108 mAh g^{-1} at 10 A g^{-1}, which was 81.8% of that at current densities of 5 A g^{-1} [40], see Figure 2b. The principle of the device involves two steps single-electron redox processes, see Figure 2c. The development of this capacitor provides some enlightenment for future applications of COF electrodes in supercapacitors.

4.1.2. TEMPO-Based COF Electrode Materials

Post-synthetic modification is also a strategy to introduce redox groups into COFs. Jiang et al., modified NiP-COF using TEMPO by click reaction and the obtained NiP-COF achieved a decent energy storage capacity: the capacitances of NiP-100-COF and NiP-50-COF were 167 and 124 F g^{-1} at 100 mA g^{-1}, respectively [41].
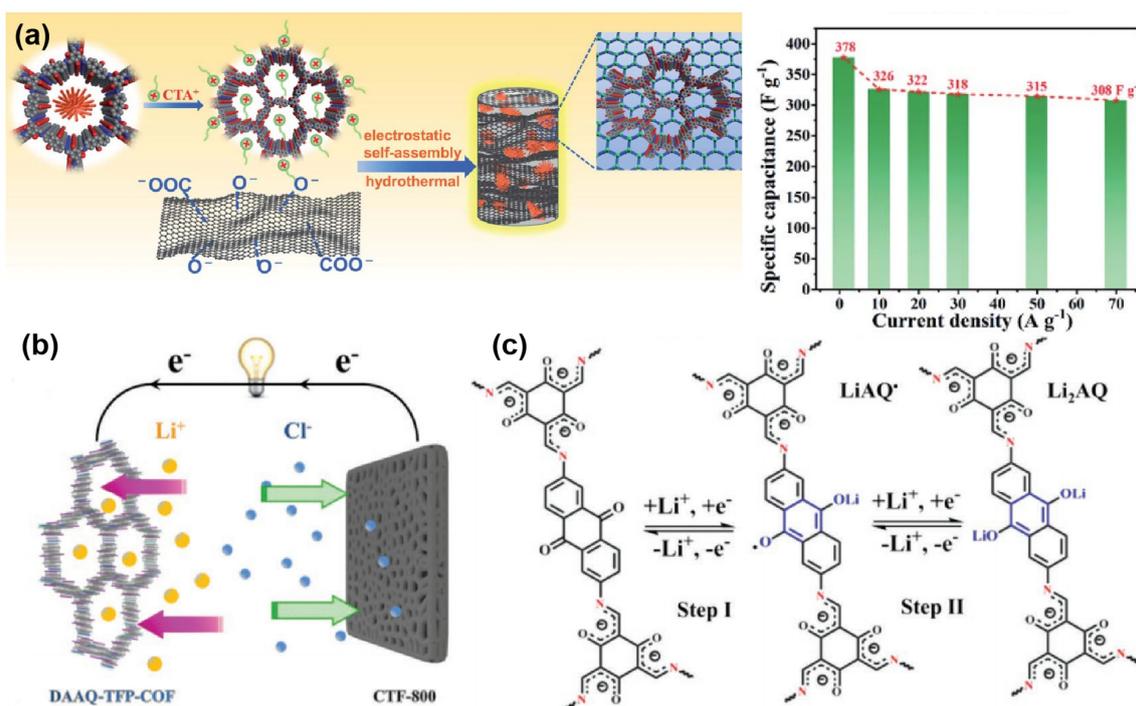
Figure 2. (**a**) Schematic of the synthesis procedure for the D−COF−GA composite and specific capacitances versus the current densities of D−COF/GA from 1 to 70 A g^{-1}. Reprinted with permission from Ref. [39]. Copyright 2021, Royal Society of Chemistry. (**b**) Schematic diagram of the DT−COF//CTF−800 ALIC device; (**c**) The principle of the device involves two steps single−electron redox processes. Reprinted with permission from Ref. [40]. Copyright 2022, WILEY-VCH.

4.1.3. Quinone-Based COF Electrode Materials

Quinone has been used to construct COF-based electrode materials. In 2016, Banerjee et al., synthesized TpPa-COF and TpBD-COF for supercapacitor applications.

H_2Q-moieties were integrated into the matrix of stable 2D COFs. The electrode using TpPa-COF showed a specific capacitance of 214 F g^{-1} at a current density of 200 mA g^{-1}. Moreover, TpPa-COF had 66% specific capacitance retention (10,000 cycles) in the three electrode structures, compared with 88% in the two electrode configurations (also 10,000 cycles) [42]. Meanwhile, the TaPa-Py COF electrode showed a good cycle ability after 6000 cycles with a capacitance retention of 92% in [43]. Recently, a 2D COFs@graphene hybrids [37] showed a 599 F g^{-1} capacitance [44]. This shows the great potential of graphene/COF hybrid materials for supercapacitor applications.

4.1.4. Triazine-Based COF Electrode Materials

Yang and Guo et al. synthesized PM-COF via a condensation reaction. Since both MA and PDA are high nitrogen content materials, the nitrogen content of PM-COF reached 47.87%, resulting in an electronic conductivity as high as 3.34×10^{-2} S. This triazine-based COF, made of cheap monomers, showed specific capacitance of 355 F g^{-1} at 1 A g^{-1} (Figure 3a) [45].

In addition, porous carbon with nitrogen-doping (N-PC) was prepared by carbonization using a triazinyl COF through the Friegel-Crafts reaction in [46]. Due to the electron pairs containing a single heteroatom, the N-PC showed a specific capacitance of 112 F g^{-1} at 1.0 A g^{-1} (Figure 3b). A lot of halogen-functionalized strategy was deployed to improve the electrochemical performance of CTFs and excellent results were acquired [47].
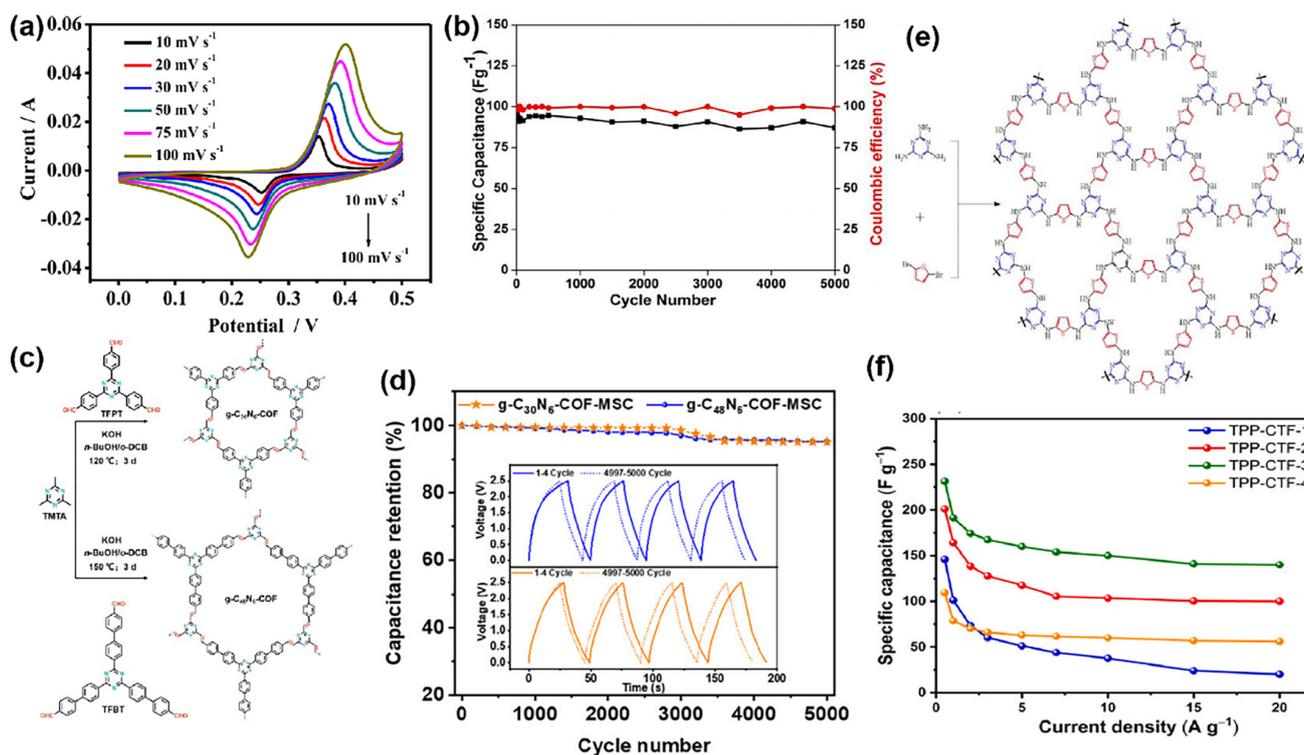
Figure 3. (**a**) CV curves at different scan rates (10, 20, 30, 50, 75, and 100 mV s^{-1}) with saturated calomel electrode as the reference electrode. Reprinted with permission from Ref. [45]. Copyright 2019, American Chemical Society. (**b**) Cycle stability and Coulombic efficiency of the N–PC at a current density of 2 A g^{-1}. Reprinted with permission from Ref. [46]. Copyright 2020, Springer. (**c**) Synthetic routes to g–C30N6–COF and g–C48N6–COF; (**d**) Cycling stability of g–C30N6–COF–MSC and g_x0002_C48N6-COF-MSC measured at 1.2 mA cm^{-2} under the voltage window of 2.5 V (inset shows the first four cycles and the last four cycles GCD curves). Reprinted with permission from Ref. [48]. Copyright 2020, Elsevier. (**e**) Synthetic routes to g–C30N6–COF and g–C48N6–COF. Reprinted with permission from Ref. [49]. Copyright 2020, Elsevier. (**f**) Specific capacitances of TPP–CTF–1, TPP–CTF–2, TPP–CTF–3, and TPP–CTF–4 at various current densities. Reprinted with permission from Ref. [50]. Copyright 2022, Elsevier.

Olefin-linked 2D COFs are also emerging as promising electrode materials, due to their splendid π-electron communication and high stability. Zhang et al. [48] prepared G$_{30}$-COF and G$_{48}$-COF, with tritopic triazine-cored aldehydes, via Knoevenagel condensation (Figure 3c). By using the ionogel electrolyte of EMIMBF$_4$/PVDF-HFP (EMIMBF$_4$ = 1-ethyl-3-methylimidazolium tetraflfluoroborate, PVDF-HFP = Poly vinylidene fluoride-co-hexafluoropropylene), G$_{30}$-COF-MSCs (MSCs = micro-supercapacitors) not only delivered high capacitances of 44.3 F g^{-2} but also had good capacitance retention of 95% at 5000 cycles (Figure 3d).

Another triazine-based COF material, named D-M-COF [49], was synthesized to be used as electrode material of a supercapacitor. The D-M-COF was obtained from DBT and melamine via C-N coupling reaction (Figure 3e). The supercapacitor assembled with D-M-COF showed good capacitive behavior. The device delivered an outstanding stability (capacitance retention of 83% after 30,000 cycle). The specific capacitance of the D-M-COF electrode showed a capacitance of 407 F g^{-1} at 1 A g^{-1}. The specific capacitance of a novel class of pyridine-based COF (TPP-CTFs) [50] was 231 F g^{-1} at 0.5 A g^{-1} (Figure 3f). Especially notable was the fact that TPP-CTF-3 featured high stability with 99.18% capacitance retention after 2000 cycles at 10 A g^{-1}, which suggested industrial applicability.

4.1.5. Conductive COF Electrode Materials

As we all know, the low electrical conductivity of COFs is the main reason that their application in supercapacitors has been impeded. Researchers have tried to build conductive COFs for use in supercapacitors. In 2017, Sheberla and coworkers reported a highly conductive MOF, $[Ni_3(HITP)_2]_n$. The planar Ni(II) coordination was the main reason for its high conductivity. Inspired by that work, Yan et al. designed and synthesized a Ni(II)-Salphen COF. The electrical conductivity of Ni-COF powder was 1.3×10^{-2} S cm^{-1}, while the COF without Ni^{2+} (Ni$_0$-COF) was only 8.4×10^{-6} S cm^{-1}. In a three-electrode system, the specific capacitance of the Ni-COF electrode was 1257 F g^{-1} at 1 A g^{-1} [51] (Figure 4a).
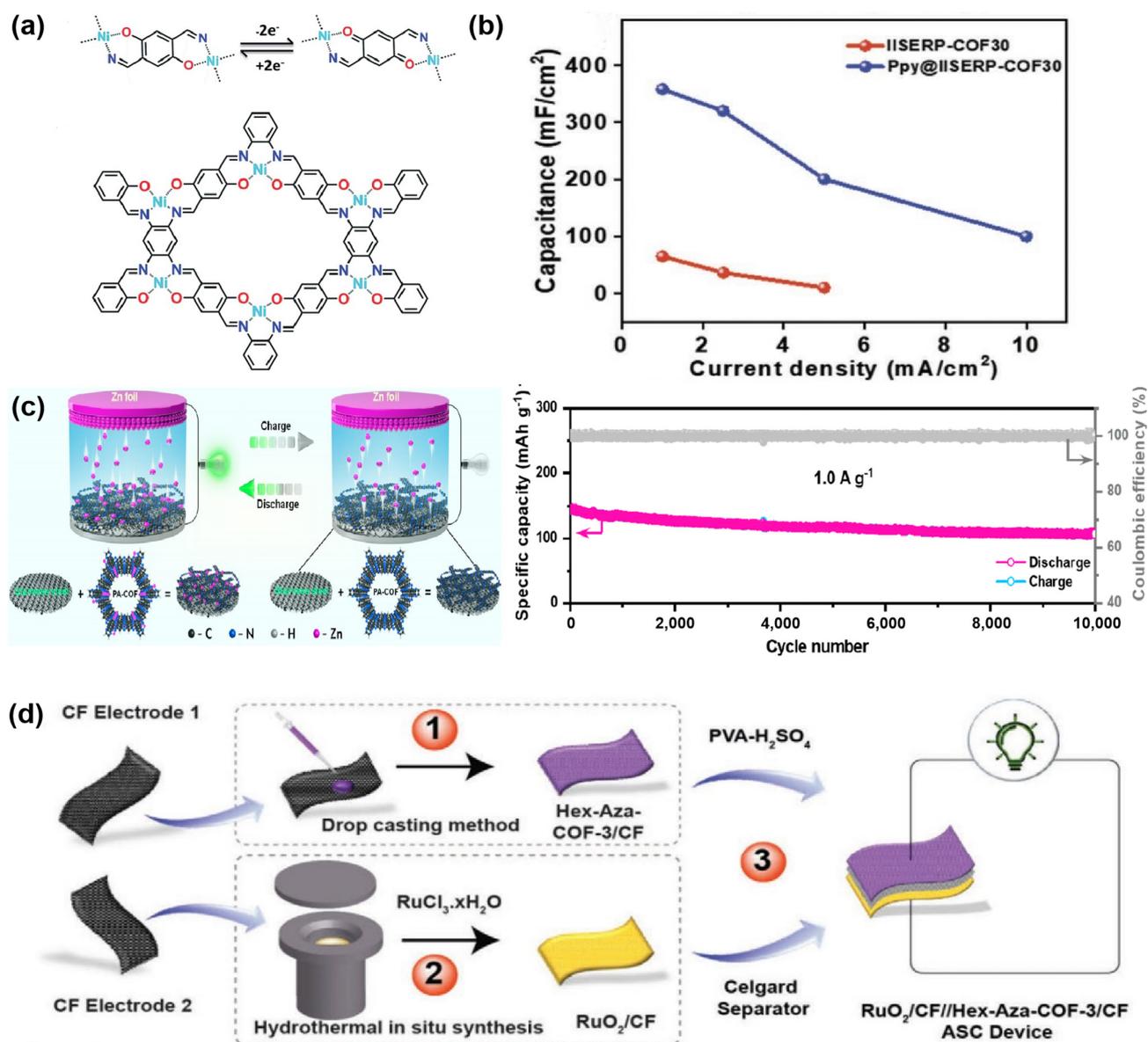

Figure 4. (**a**) The possible energy storage/conversion mechanism and $\pi-$conjugated structure of Ni$-$COF. Reprinted with permission from Ref. [51]. Copyright 2019, Royal Society of Chemistry.

(**b**) Capacitance variation of COF and Ppy@COF at different current densities. Reprinted with permission from Ref. [52]. Copyright 2022, WILEY-VCH. (**c**) Schematic configuration of PA−COF∥1.0 M $ZnSO_4$∥Zn metal ZIS. Electrochemical behavior of PACOF in 1.0 M $ZnSO_4$ electrolyte within a potential window of 0.2−1.6 V. The remarkable cycling stability of PA−COF at a current density of 1.0 A g^{-1}. Reprinted with permission from Ref. [53]. Copyright 2019, American Chemical Society. (**d**) Schematic representation illustrating the fabrication of RuO_2//Hex−Aza−COF−3 ASC device. Reprinted with permission from Ref. [54]. Copyright 2020, WILEY−VCH.

The Ppy@COF formed by incorporating conductive polypyrrole (Ppy) chains into a polyimide COF showcased promising prospects as a carbon-free energy storage material [52]. The capacitance of Ppy@COF electrode was 358 mF cm^{-2} at 1 mA cm^{-2} (Figure 4b).

4.1.6. Phenanthroline-Based COF Electrode Materials

In 2020, a new strategy to synthesize PA-COF as cathode in zinc-ion supercapacitors (ZISs), via the condensation reaction [53] was first introduced, and showed a capacity of 247 mAh g^{-1} at a low current density of 0.1 A g^{-1}. Due to the phenanthroline functional group in PA-COF, which is the active storage site of zinc ions, the capacity attenuation of PA-COF was only 0.38% in the course of 10,000 cycles (at a current density of 1 A g^{-1}) (Figure 4c).

The Hex-Aza-COF [54], containing redox functional moieties and a hetero-nitrogen fusion π-conjugated system, was designed, prepared and exploited as a negative electrode in asymmetric supercapacitors (ACSs) (Figure 4d). As mentioned above, they achieved high specific capacitances of 585 F g^{-1} and 663 F g^{-1} (in the three-electrode configuration), respectively.

4.1.7. Customized-Type COF Electrode Materials

Triphenylphosphine (PPh_3) was first introduced into COFs and successfully utilized as electrode material for pseudo-capacitors in [55]. The Phos-COF-1, was synthesized by the traditional solvothermal method, and exhibited a specific capacitance of 100 F g^{-1} when the current density was 1 A g^{-1} and showed high cyclability with 90% capacitance retention after 5000 charge/discharge cycles. Further studies to improve the properties of phosphine-based COF materials are still in progress. PI-COF [56], also synthesized by the solvothermal method, showed outstanding electrochemical performance applied to supercapacitors. PI-COF exhibited an energy density of 35.7 W/kg at a power density of 250 W/kg in 1 mol/L lithium bis(trifluoromethanesulfonyl)imide [$LiN-(CF_3SO_2)_2$, LITFSI] electrolyte. Remarkably, at a high current density of 4 A g^{-1}, the capacitance of PI-COF was retained at 79% (112 F g^{-1}), even after 30,000 cycles. A kind of exfoliated mesoporous (3.4 nm) 2D covalent organic framework COF (e-COF) with an A-A stacking mode, favorable BET surface area (up to 1170 m^2 g^{-1}) and high stability was exploited into a thin layer structure with an average thickness of 22 nm by the chemically exfoliated method for double-layer charge storage [57].

The e-COF achieved an areal capacitance of 5.46 mF/cm^2 at a scan rate of 1000 mV/s, high gravimetric power of 55 kW/kg, and low τ_0 value of 121 ms the minimum time required to discharge more than 50% energy. Importantly, almost DL storage behavior was delivered at 30,000 mV s^{-1} and there was almost no reduced capacity after 10,000 cycles. Researchers often build composites to ameliorate the electrochemical performance of these COF-based materials. Hetero-porous bifluorenylidene-based COFs showed excellent dye adsorption behavior and good energy storage. The three electrodes exhibited high stability and robustness, and the capacitance retention rates were 97.27, 85.23 and 91.21%, respectively [58].The COF/rGO aerogel synthesized by Li et al. [59] not only showed good adsorption capacity, but could also be directly used as electrode materials for high-performance supercapacitors without adding additives or binders. Three-dimensional porous kenaf stem-derived carbon (3D-KSC)/COF-LZU1 COF-LZU-x series were synthesized and named by Lanzhou University. and polyaniline (PANI) composites were prepared

for supercapacitor application in [60]. COF-LZU1 could refine the poor thermal stability of PANI and compensated for the shortcomings of the three materials. Employing this approach, the electrical conductivity and mechanical strength of the composite were greatly ameliorated, with an area specific capacitance up to 583.0 mF cm^{-2}. The TPA-COF in [61] was prepared by the solvothermal method and also had good electrochemical performance. Meanwhile, hybrids of metal–organic framework and COF were also designed as active material in supercapacitors in [62]. The redox-active 7,7,8,8-tetracyanoquinodimethane (TCNQ) molecules were introduced into the MOF@COF pore channels via liquid-phase infiltration (Figure 5a). MOF@COF-TCNQ showed excellent energy storage as the electrodes in 1 M tetraethy lammonium tetraflfluoroborate (TEABF$_4$) contained acetonitrile (AN) electrolyte, with a real capacitance of 78.36 mF cm^{-1}, and volumetric energy density of 4.46 F cm^{-3}. As a kind of composite material, at 1 A g^{-1} PEDOT@AQ-COF showed an amazing specific capacitance of 1663 F g^{-1} [63]. In addition, DqTp-CNF and DqDaTp-CNF, with capacities of 464 mF/cm^2 and 364 mF/cm^2, were also worthy of further study in [64].

COF-based materials have great potential in the application of flexible supercapacitors. For example, Zhang et al., reported a novel strategy for the construction of extensible and flexible supercapacitors (Figure 5b). Firstly, through a simple solid-state mechanical mixing method, a β-ketoenamine-linked redox-active COF complex was constructed with hydroxyl-terminated hyperbranched polymer (OHP) as template. Then, to construct the COF@OHP@CNTF composite membrane (CHCM), the COF@OHP complex was impregnated on microporous conductive carbon nanotube films (CNTFs). The composite film could be used as a CHCM electrode for flexible and scalable supercapacitors [65]. The CHCM electrode showed a gravimetric capacitance of 249 F g^{-1}, cyclic stability of 80% after 10,000 times of cycling in 1 M H$_3$PO$_4$ electrolyte, tensile strength of 180 MPa and elongation of 10%, which provided a potentially wide prospect for the application of COF materials in wearable flexible supercapacitors.

COF combined with fullerene through a nano-templating method achieved electrode material for supercapacitors [66]. C$_{60}$ has high electron affinity and a unique π-conjugated system. However, the lack of structural order and porosity limits their electrochemical accessibility and ion transport. Coincidentally, COFs have highly ordered porosity and crystallinity. Thus, Zhao and his coworkers designed and prepared a series of COF-templated, ordered, nano-porous C$_{60}$ ([C$_{60}$]X-COFs) through click reaction applied to asymmetric supercapacitors (ASCs) (Figure 5c). The ASC composed of [C$_{60}$]0.05-COFs could operate at a voltage window of 1.8 V, and the capacitance amazingly retained 99% after 5000 times cycles (4 A g^{-1}). In 2021, a novel class of COFs with a specific capacitance of 1443 F g^{-1} were reported. These porphyrin-tetraphenyl ethylene COFs (PT-COFs) [67] not only exhibited high crystallinity along with a large surface area of 1998 m^2 g^{-1}, but also achieved a power density of 7.3 kW kg^{-1} and 91% specific capacitance retention at 5 A g^{-1}. The existence of the porphyrin unit in the framework endowed the PT-COFs with excellent redox activity in acidic media (Figure 5d).
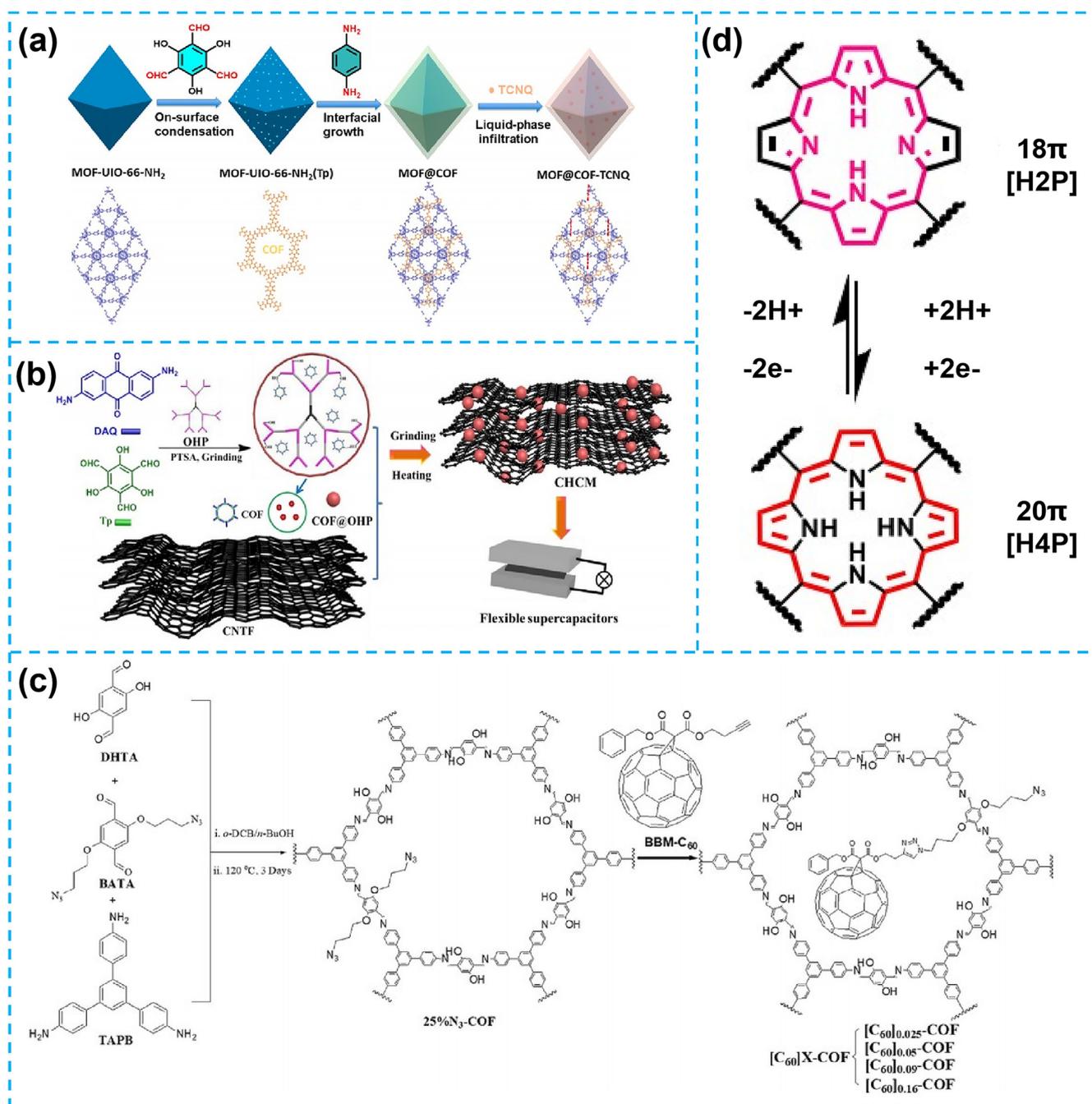
Figure 5. (**a**) Schematic of the synthesis route for MOF@COF−TCNQ hybrids. Reprinted with permission from Ref. [62]. Copyright 2021, American Chemical Society. (**b**) CHCM synthesis and application to flexible supercapacitors. Reprinted with permission from Ref. [65]. Copyright 2020, Elsevier. (**c**) Schematic illustration of the template synthesis of [C60]X−COFs. Reprinted with permission from Ref. [66]. Copyright 2021, Elsevier. (**d**) Plausible redox activity by the porphyrin core inside PTCOF; [H2P] and [H4P] indicate the pristine porphyrin and the reduced form of [H2P] after protonation, respectively. Reprinted with permission from Ref. [67]. Copyright 2021, American Chemical Society.

4.2. COF-Based Solid-State Device

In order to solve the problem of weak activity of redox groups in the COF-derived solid-state capacitors at a high current density, three COFs with pyridyl-lined micropores were developed [68]. IISERP-COF10, IISERP-COF11, IISERP-COF12 were constructed with COF

using phenol-, resorcinol-, and phloroglucinol-derived trialdehydes, respectively. When assembled into a solid-state capacitor, the three kinds of COF all showed decent energy storage ability (Figure 6a). Among them, IISERP-COF10 (1-OH) exhibited a low capacitance (~92 mF cm^{-2} at 0.5 mA cm^{-2}), and IISERP-COF12 (3-OH) retained 95% of its initial capacity (Figure 6b). Moreover, the three IISERP-COF10 were connected in series to form a solid-state device that enabled the light emitting diode [54] to glow for approximately 1 min. However, the capacity of this solid-state capacitor was inferior to that of the solid-state device assembled by COF-CNF (167 mF/cm^2) at the same current density of 0.5 mA cm^{-2} in [64]. In 2018, Banerjee et al. fabricated a symmetric solid-state supercapacitor by applying two 1 cm^2 COF thin sheets (ultra-stable TPOME-DAQ) with 2M H_2SO_4/PVA as the electrolyte and achieved an area capacitance of 84 mF cm^{-2} (8.8 F g^{-1}) [69]. The energy density and power density were ~2.9 μWh/cm^2 and 61.8 μW/cm^2, respectively. In 2021, it was reported that the conductivity of IISERP-COF25 was 3.16×10^{-4} S cm^{-2} and revealed a high gravimetric capacitance (57 ± 8 F g^{-1}) and a real capacitance (~270 ± 11 mF/cm^2) when fabricated as a practical solid-state device, while using an electrolyte containing KI as the redox-active additive [70]. The addition of KI to the H_2SO_4 electrolyte yielded outstanding enhancement in solid-state gravimetric specific capacitance (Figure 6c). Meanwhile, the imine-COF demonstrated 89% of its initial capacity retention even after 10,000 cycles.
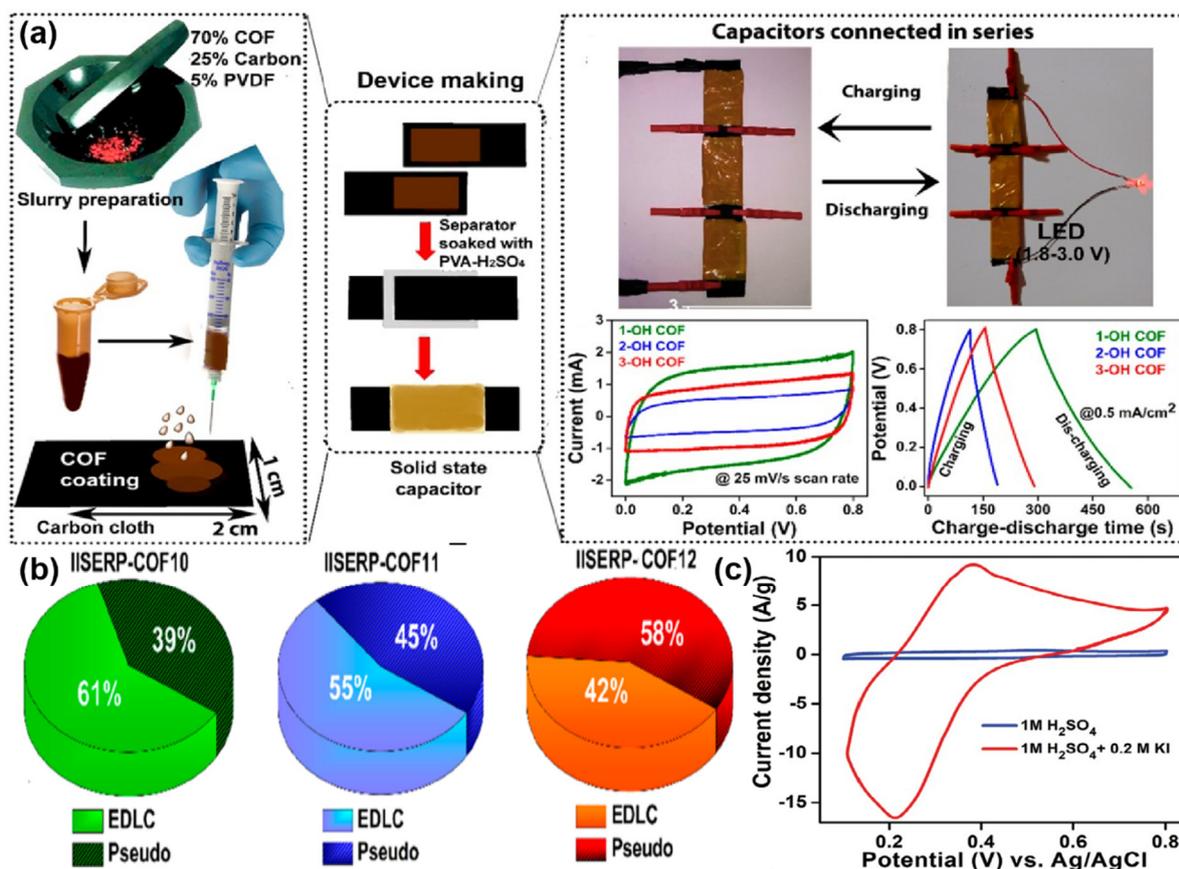

Figure 6. (**a**) The process of solid-state device preparation, CVs measured under solid-state conditions for the IISERP–COF10, IISERP–COF11, IISERP–COF12 and galvanostatic charge–discharge curves; (**b**) Graphical representation of capacitance contribution comes from EDLC and pseudo–activity of pyridine-rich COFs. Reprinted with permission from Ref. [68]. Copyright 2019, American Chemical Society. (**c**) Comparative CV plots of the COF–derived solid–state device (geometrical surface area = 1 cm^2) measured using 1 m H_2SO_4 and 1 m H_2SO_4 + 0.2 mKI as electrolyte @500 mV s^{-1} scan rate with a 10 mg total loading. Reprinted with permission from Ref. [70]. Copyright 2021, WILEY–VCH.

5. Summary and Outlook

When used as the electrode material for supercapacitors, COF material has garnered much attention as a novel type of porous material. High porosity, high crystallinity, a clear skeleton, and the capacity to be functionally designed make COFs very promising in the field of energy storage. Recently, it has become clear that COF can be used as a candidate material for high-performance supercapacitors. This review began by outlining the features of COFs in the context of their use in supercapacitors and their methods of synthesis. The use of previously published COF materials in supercapacitors was next evaluated with regard to electrode materials and solid-state devices. Finally, essential aspects and potential difficulties were discussed and the exceptional performance characteristics of COFs illustrated from a supercapacitor standpoint. This review also forecasts the future course of COF-based supercapacitor development.

However, the following issues still exist for COF-based supercapacitors: (1) A lot of COF-based electrode materials are investigated using three electrode systems, which might not be ideal. They should be researched more thoroughly and put to use in real-world situations. (2) To increase capacitance, one should balance density, porosity, pore size, and other factors, in order to get the greatest ion transport and storage performance. It is not a good idea to focus just on increasing specific surface area. (3) Due to their deep active sites, several COF-based electrode materials are challenging to completely exploit. (4) Insufficient electrical conductivity remains an issue. (5) More research is needed on the energy storage mechanism of some electrode materials based on COFs.

COFs have good thermal and chemical stability, as well as very high crystallinity. As a result, the primary goal of COFs' employment in supercapacitors in recent years has been to increase their electrical conductivity. The conductivity of COFs can be enhanced by increasing the conjugation degree of the skeleton, modification after synthesis, or hybridization with conductive materials. Additionally, modifying COFs with redox-active groups to increase their ability to store energy has become a popular tactic in recent years. We gave an overview of the recent remarkable performance of CF-based electrode materials (Tables 1 and 2). It is clear that COFs containing DAAQ, triazine-based COFs, and conductive COFs have received the most attention and have been used the most, while other COF materials still require development and more research. COF-derived electrode materials to be applied to practical supercapacitors with capacities higher than 100 F g^{-1} are the following: DAAQ-GA-COFs [39] (378 F g^{-1}), TpPa-(OH)$_2$ [42] (214 F g^{-1}), TpTa-Py COF [43] (102 F g^{-1}), Ni-COF [51] (417 F g^{-1}), FCTF [47] (148 F g^{-1}), PI-COF [56] (163 F g^{-1}), COF-rGO [59] (269 F g^{-1}), DqDaTp-CNF [64] (167 F g^{-1}). We are looking forward to more applications of COF-derived materials in supercapacitors.

Table 1. COF-derived electrode materials and their electrochemical performance in three-electrode system.

Electrode System	Electrode	Specific Capacitance	Current Density/ Scan Rate	Electrolyte	Retention (Cycle)	SBET (m²/g)	Ref.
three-electrode	DT-BASED COF	40 ± 9 F g^{-1}	0.1 A g^{-1}	1 M H$_2$SO$_4$	5000	425	[36]
	DAB-TFP-COF	15 ± 6 F g^{-1}			——	365	
	DAAQ-TFP COF thin films	3 mF cm^{-2}	0.15 mA cm^{-2}	1 M H$_2$SO$_4$	93% (5000)	——	[37]
	[TEMPO]100%-NiP-COF	167 F g^{-1}	0.1 A g^{-1}	0.1 M (C$_4$H$_9$)$_4$ NClO$_4$	—	5.2	[41]
	[TEMPO]50%-NiP-COF	124 F g^{-1}			100	264	
	TpTa-Py COF	209 F g^{-1}	0.5 A g^{-1}	1 M H$_2$SO$_4$	—	687	[43]
	Ni-COF	1257 F g^{-1}	1 A g^{-1}	3 M KOH	94% (10,000)	362	[51]
	Ppy@COF	1983 mF g^{-1}	1 A g^{-1}	1 M PVA -H$_2$SO$_4$	98% (2800)	657	[52]

Table 1. *Cont.*

Electrode System	Electrode	Specific Capacitance	Current Density/ Scan Rate	Electrolyte	Retention (Cycle)	SBET (m^2/g)	Ref.
	Hex-Aza-COF-1	220 F g^{-1}	1 A g^{-1}	1 M H$_2$SO$_4$		85	[54]
	Hex-Aza-COF-2	585 F g^{-1}				96	
	Hex-Aza-COF-3	663 F g^{-1}				124	
	N-PC	112 F g^{-1}	1 A g^{-1}	6 M KOH	88.4% (5000)	711	[46]
	COF@OHP @CNTF	249 F g^{-1}	30 mV s^{-1}	1 M H$_3$PO$_4$	80% (10,000)	167	[65]
	Phos-COF-1	100 F g^{-1}	1 A g^{-1}	3 M Na$_2$SO$_4$	90% (5000)	818	[55]
	MOF@ COF-TCNQ	78.36 F cm^{-1}	0.2 A g^{-1}	1 M TEABF4 /AN	86.4% (2000)	265	[62]
	PT-COF	1443 F g^{-1}	1 A g^{-1}	0.5 M H$_2$SO$_4$	91% (3000)	1998	[67]
	TpOMe-DAQ	169 F g^{-1}	3.3 mA cm^{-2}	3 M H$_2$SO$_4$	65% (50,000)	1531	[69]

Table 2. COF-derived electrode materials and their electrochemical performance in practical device (two-electrode system).

Electrode System	Electrode	Specific Capacitance	Current Density/ Scan Rate	Electrolyte	Retention (Cycle)	SBET (m^2/g)	Energy Density (Wh/kg)	Power Density (W/kg)	Ref.
two-electrode	DAAQ-GA-COFs //GA	378 F g^{-1}	1 A g^{-1}	1 M H$_2$SO$_4$	88.9% (20,000)	425.3	30.5	700	[39]
	TpPa-(OH)$_2$	214 ± 1 F g^{-1}	0.2 A g^{-1}	1 M phosphate buffer	88% (10,000)	369	——	——	[42]
	TpTa-Py COF	102 F g^{-1}	0.5 A g^{-1}	1 M H$_2$SO$_4$	92% (6000)	687	9.06	100	[43]
	Ni-COF//AC	417 F g^{-1}	1 A g^{-1}	3 M KOH	——	362	130	839	[51]
	RuO$_2$// Hex-Aza-COF-3	64 F g^{-1}	1 A g^{-1}	1 M H$_2$SO$_4$	89% (7500)	——	23.3	661.2	[54]
	PA-COF//Zn	247 mAh g^{-1}	0.1 A g^{-1}	1 M ZnSO$_4$	74% (10,000)	——	——	——	[53]
	FCTF//AC	148 F g^{-1}	1 A g^{-1}	1 M H$_2$SO$_4$	98.8% (10,000)	829	46.3	975	[47]
	PI-COF//PI-COF	163 F g^{-1}	0.5 A g^{-1}	1 M LITFSI	84.1% (30,000)	375	35.7	250	[56]
	COF-rGO	269 F g^{-1}	0.5 A g^{-1}	0.5 M H$_2$SO$_4$	96% (5000)	246	——	——	[59]
	[C60]0.05-COF //rGO	47.6 F g^{-1}	1 A g^{-1}	1 M Na$_2$SO$_4$	99% (5000)	320	21.4	900	[66]

Regarding the application of COF materials in supercapacitors, the following key points are summarized:(1) Adjust the structure of COFs to obtain rich surface properties and electrochemical properties; (2) Based on the functional design of COF composite materials, they are endowed with good mass transfer, high conductivity and structural stability; (3) Through theoretical calculation, or machine learning and other methods, we can deeply understand their energy storage mechanism and reveal their potential electrochemical mechanism; (4) The functional design of the integrated electrode integrates the intelligent supercapacitor into a wider range of application scenarios, such as intelligent wearable devices, flexible electronic devices, etc.

Designing and synthesizing exceptional materials with electrochemical and stable behavior for supercapacitors has become a popular research theme. Therefore, during the construction of supercapacitors, developing more high-performance COF-based materials is of great significance to our society and world. After this review and research, we predict that, in the next few years, there will be more and more research on COF-based materials and outstanding results will be achieved. COF is going to play an important role in the material source of supercapacitors. We think that COF materials can be used to build more high-performance and affordable supercapacitors in the future, which will eventually lead to their commercialization.

References

1. Cote, A.P.; Benin, A.I.; Ockwig, N.W.; O'Keeffe, M.; Matzger, A.J.; Yaghi, O.M. Porous, crystalline, covalent organic frameworks. *Science* **2005**, *310*, 1166–1170. [CrossRef]
2. Bao, W.; Wang, R.; Sun, K.; Qian, C.; Zhang, Y.; Li, J. Interface Crystallographic Optimization of Crystal Plane for Stable Metallic Lithium Anode. *ACS Appl. Mater. Interfaces* **2022**, *14*, 38696–38705. [CrossRef]
3. Wang, R.; Li, M.; Sun, K.; Zhang, Y.; Li, J.; Bao, W. Element-Doped Mxenes: Mechanism, Synthesis, and Applications. *Small* **2022**, *18*, 2201740. [CrossRef]
4. Wang, R.; Liu, H.; Zhang, Y.; Sun, K.; Bao, W. Integrated Photovoltaic Charging and Energy Storage Systems: Mechanism, Optimization, and Future. *Small* **2022**, *18*, 2203014. [CrossRef] [PubMed]
5. Wang, R.; Sun, K.; Liu, H.; Qian, C.; Li, M.; Zhang, Y.; Bao, W. Integrating a redox-coupled $FeSe_2$/N–C photoelectrode into potassium ion hybrid capacitors for photoassisted charging. *J. Mater. Chem. A* **2022**, *10*, 11504–11513. [CrossRef]
6. Wang, R.; Sun, K.; Zhang, Y.; Qian, C.; Bao, W. Dimensional optimization enables high-performance capacitive deionization. *J. Mater. Chem. A* **2022**, *10*, 6414–6441. [CrossRef]
7. Bao, W.; Wang, R.; Li, B.; Qian, C.; Zhang, Z.; Li, J.; Liu, F. Stable alkali metal anodes enabled by crystallographic optimization—A review. *J. Mater. Chem. A* **2021**, *9*, 20957–20984. [CrossRef]
8. Wang, R.; Zhang, Y.; Sun, K.; Qian, C.; Bao, W. Emerging green technologies for recovery and reuse of spent lithium-ion batteries—A review. *J. Mater. Chem. A* **2022**, *10*, 17053–17076. [CrossRef]
9. Fang, Q.; Zhuang, Z.; Gu, S.; Kaspar, R.B.; Zheng, J.; Wang, J.; Qiu, S.; Yan, Y. Designed synthesis of large-pore crystalline polyimide covalent organic frameworks. *Nat. Commun.* **2014**, *5*, 4503. [CrossRef]
10. Feng, X.; Ding, X.; Jiang, D. Covalent organic frameworks. *Chem. Soc. Rev.* **2012**, *41*, 6010–6022. [CrossRef]
11. Pang, Z.-F.; Zhou, T.-Y.; Liang, R.-R.; Qi, Q.-Y.; Zhao, X. Regulating the topology of 2D covalent organic frameworks by the rational introduction of substituents. *Chem. Sci.* **2017**, *8*, 3866–3870. [CrossRef]
12. Tilford, R.W.; Mugavero, S.J., III; Pellechia, P.J.; Lavigne, J.J. Tailoring microporosity in covalent organic frameworks. *Adv. Mater.* **2008**, *20*, 2741–2746. [CrossRef] [PubMed]
13. Zhang, G.; Tsujimoto, M.; Packwood, D.; Nghia Tuan, D.; Nishiyama, Y.; Kadota, K.; Kitagawa, S.; Horike, S. Construction of a Hierarchical Architecture of Covalent Organic Frameworks via a Postsynthetic Approach. *J. Am. Chem. Soc.* **2018**, *140*, 2602–2609. [CrossRef] [PubMed]
14. Zhou, T.-Y.; Xu, S.-Q.; Wen, Q.; Pang, Z.-F.; Zhao, X. One-Step Construction of Two Different Kinds of Pores in a 2D Covalent Organic Framework. *J. Am. Chem. Soc.* **2014**, *136*, 15885–15888. [CrossRef]
15. Ding, S.-Y.; Wang, W. Covalent organic frameworks (COFs): From design to applications. *Chem. Soc. Rev.* **2013**, *42*, 548–568. [CrossRef]
16. Huang, N.; Wang, P.; Jiang, D. Covalent organic frameworks: A materials platform for structural and functional designs. *Nat. Rev. Mater.* **2016**, *1*, 16068. [CrossRef]
17. Kandambeth, S.; Dey, K.; Banerjee, R. Covalent Organic Frameworks: Chemistry beyond the Structure. *J. Am. Chem. Soc.* **2019**, *141*, 1807–1822. [CrossRef]
18. Meng, Y.; Luo, Y.; Shi, J.L.; Ding, H.; Lang, X.; Chen, W.; Zheng, A.; Sun, J.; Wang, C. 2D and 3D Porphyrinic Covalent Organic Frameworks: The Influence of Dimensionality on Functionality. *Angew. Chem. Int. Ed* **2020**, *59*, 3624–3629. [CrossRef]
19. Li, J.; Jing, X.; Li, Q.; Li, S.; Gao, X.; Feng, X.; Wang, B. Bulk COFs and COF nanosheets for electrochemical energy storage and conversion. *Chem. Soc. Rev.* **2020**, *49*, 3565–3604. [CrossRef] [PubMed]

20. Waller, P.J.; Gandara, F.; Yaghi, O.M. Chemistry of Covalent Organic Frameworks. *Acc. Chem. Res.* **2015**, *48*, 3053–3063. [CrossRef]

21. Hussain, I.; Iqbal, S.; Hussain, T.; Cheung, W.L.; Khan, S.A.; Zhou, J.; Ahmad, M.; Khan, S.A.; Lamiel, C.; Imran, M.; et al. Zn–Co-MOF on solution-free CuO nanowires for flexible hybrid energy storage devices. *Mater. Today Phys.* **2022**, *23*, 100655. [CrossRef]

22. Sahoo, S.; Dhakal, G.; Kim, W.K.; Shim, J.-J. Ternary Nanohybrid of $Ni_3S_2/CoMoS_4/MnO_2$ on Nickel Foam for Aqueous and Solid-State High-Performance Supercapacitors. *Nanomaterials* **2022**, *12*, 1945. [CrossRef]

23. Sahoo, S.; Kumar, R.; Joanni, E.; Singh, R.K.; Shim, J.-J. Advances in pseudocapacitive and battery-like electrode materials for high performance supercapacitors. *J. Mater. Chem. A* **2022**, *10*, 13190–13240. [CrossRef]

24. Wang, H.; Zeng, Z.; Xu, P.; Li, L.; Zeng, G.; Xiao, R.; Tang, Z.; Huang, D.; Tang, L.; Lai, C.; et al. Recent progress in covalent organic framework thin films: Fabrications, applications and perspectives. *Chem. Soc. Rev.* **2019**, *48*, 488–516. [CrossRef] [PubMed]

25. Colson, J.W.; Woll, A.R.; Mukherjee, A.; Levendorf, M.P.; Spitler, E.L.; Shields, V.B.; Spencer, M.G.; Park, J.; Dichtel, W.R. Oriented 2D Covalent Organic Framework Thin Films on Single-Layer Graphene. *Science* **2011**, *332*, 228–231. [CrossRef]

26. Chandra, S.; Kandambeth, S.; Biswal, B.P.; Lukose, B.; Kunjir, S.M.; Chaudhary, M.; Babarao, R.; Heine, T.; Banerjee, R. Chemically Stable Multilayered Covalent Organic Nanosheets from Covalent Organic Frameworks via Mechanical Delamination. *J. Am. Chem. Soc.* **2013**, *135*, 17853–17861. [CrossRef]

27. Biswal, B.P.; Chandra, S.; Kandambeth, S.; Lukose, B.; Heine, T.; Banerjeet, R. Mechanochemical Synthesis of Chemically Stable Isoreticular Covalent Organic Frameworks. *J. Am. Chem. Soc.* **2013**, *135*, 5328–5331. [CrossRef] [PubMed]

28. Rao, M.R.; Fang, Y.; De Feyter, S.; Perepichka, D.F. Conjugated Covalent Organic Frameworks via Michael Addition-Elimination. *J. Am. Chem. Soc.* **2017**, *139*, 2421–2427. [CrossRef] [PubMed]

29. Wang, S.; Wang, Q.; Shao, P.; Han, Y.; Gao, X.; Ma, L.; Yuan, S.; Ma, X.; Zhou, J.; Feng, X.; et al. Exfoliation of Covalent Organic Frameworks into Few-Layer Redox-Active Nanosheets as Cathode Materials for Lithium-Ion Batteries. *J. Am. Chem. Soc.* **2017**, *139*, 4258–4261. [CrossRef]

30. Mu, X.; Zhan, J.; Feng, X.; Yuan, B.; Qiu, S.; Song, L.; Hu, Y. Novel Melamine/o-Phthalaldehyde Covalent Organic Frameworks Nanosheets: Enhancement Flame Retardant and Mechanical Performances of Thermoplastic Polyurethanes. *ACS Appl. Mater. Interfaces* **2017**, *9*, 23017–23026. [CrossRef]

31. Bao, W.; Wang, R.; Qian, C.; Zhang, Z.; Wu, R.; Zhang, Y.; Liu, F.; Li, J.; Wang, G. Porous Heteroatom-Doped Ti3C2Tx MXene Microspheres Enable Strong Adsorption of Sodium Polysulfides for Long-Life Room-Temperature Sodium–Sulfur Batteries. *ACS Nano* **2021**, *15*, 16207–16217. [CrossRef] [PubMed]

32. Wang, R.; Li, M.; Zhang, Y.; Sun, K.; Bao, W. Atomic surface modification strategy of MXene materials for high-performance metal sulfur batteries. *Int. J. Energy Res.* **2022**, *46*, 11659–11675. [CrossRef]

33. Wang, C.; Dong, H.; Hu, W.; Liu, Y.; Zhu, D. Semiconducting pi-conjugated systems in field-effect transistors: A material odyssey of organic electronics. *Chem. Rev.* **2012**, *112*, 2208–2267. [CrossRef]

34. Jin, S.; Supur, M.; Addicoat, M.; Furukawa, K.; Chen, L.; Nakamura, T.; Fukuzumi, S.; Irle, S.; Jiang, D. Creation of Superhetero-junction Polymers via Direct Polycondensation: Segregated and Bicontinuous Donor-Acceptor pi-Columnar Arrays in Covalent Organic Frameworks for Long-Lived Charge Separation. *J. Am. Chem. Soc.* **2015**, *137*, 7817–7827. [CrossRef]

35. Sun, B.; Zhu, C.-H.; Liu, Y.; Wang, C.; Wan, L.-J.; Wang, D. Oriented Covalent Organic Framework Film on Graphene for Robust Ambipolar Vertical Organic Field-Effect Transistor. *Chem. Mater.* **2017**, *29*, 4367–4374. [CrossRef]

36. DeBlase, C.R.; Silberstein, K.E.; Truong, T.-T.; Abruña, H.D.; Dichtel, W.R. β-Ketoenamine-Linked Covalent Organic Frameworks Capable of Pseudocapacitive Energy Storage. *J. Am. Chem. Soc.* **2013**, *135*, 16821–16824. [CrossRef] [PubMed]

37. DeBlase, C.R.; Hernandez-Burgos, K.; Silberstein, K.E.; Rodriguez-Calero, G.G.; Bisbey, R.P.; Abruna, H.D.; Dichtel, W.R. Rapid and Efficient Redox Processes within 2D Covalent Organic Framework Thin Films. *ACS Nano* **2015**, *9*, 3178–3183. [CrossRef]

38. Mulzer, C.R.; Shen, L.; Bisbey, R.P.; McKone, J.R.; Zhang, N.; Abruna, H.D.; Dichtel, W.R. Superior Charge Storage and Power Density of a Conducting Polymer-Modified Covalent Organic Framework. *ACS Cent. Sci.* **2016**, *2*, 667–673. [CrossRef]

39. An, N.; Guo, Z.; Xin, J.; He, Y.; Xie, K.; Sun, D.; Dong, X.; Hu, Z. Hierarchical porous covalent organic framework/graphene aerogel electrode for high-performance supercapacitors. *J. Mater. Chem. A* **2021**, *9*, 16824–16833. [CrossRef]

40. Geng, Q.; Wang, H.; Wang, J.; Hong, J.; Sun, W.; Wu, Y.; Wang, Y. Boosting the Capacity of Aqueous Li-Ion Capacitors via Pinpoint Surgery in Nanocoral-Like Covalent Organic Frameworks. *Small Methods* **2022**, *6*, 2200314. [CrossRef]

41. Xu, F.; Xu, H.; Chen, X.; Wu, D.; Wu, Y.; Liu, H.; Gu, C.; Fu, R.; Jiang, D. Radical covalent organic frameworks: A general strategy to immobilize open-accessible polyradicals for high-performance capacitive energy storage. *Angew. Chem. Int. Ed* **2015**, *54*, 6814–6818. [CrossRef]

42. Chandra, S.; Roy Chowdhury, D.; Addicoat, M.; Heine, T.; Paul, A.; Banerjee, R. Molecular Level Control of the Capacitance of Two-Dimensional Covalent Organic Frameworks: Role of Hydrogen Bonding in Energy Storage Materials. *Chem. Mater.* **2017**, *29*, 2074–2080. [CrossRef]

43. Khattak, A.M.; Ghazi, Z.A.; Liang, B.; Khan, N.A.; Iqbal, A.; Li, L.; Tang, Z. A redox-active 2D covalent organic framework with pyridine moieties capable of faradaic energy storage. *J. Mater. Chem. A* **2016**, *4*, 16312–16317. [CrossRef]

44. Wang, C.; Liu, F.; Yan, S.; Liu, C.; Yu, Z.; Chen, J.; Lyu, R.; Wang, Z.; Xu, M.; Dai, S.; et al. Assemble 2D redox-active covalent organic framework/graphene hybrids as high-performance capacitive materials. *Carbon* **2022**, *190*, 412–421. [CrossRef]

45. Li, L.; Lu, F.; Xue, R.; Ma, B.; Li, Q.; Wu, N.; Liu, H.; Yao, W.; Guo, H.; Yang, W. Ultrastable Triazine-Based Covalent Organic Framework with an Interlayer Hydrogen Bonding for Supercapacitor Applications. *ACS Appl. Mater. Interfaces* **2019**, *11*, 26355–26363. [CrossRef] [PubMed]

46. Vargheese, S.; Dinesh, M.; Kavya, K.V.; Pattappan, D.; Rajendra Kumar, R.T.; Haldorai, Y. Triazine-based 2D covalent organic framework-derived nitrogen-doped porous carbon for supercapacitor electrode. *Carbon Lett.* **2021**, *31*, 879–886. [CrossRef]

47. Gao, Y.; Zhi, C.; Cui, P.; Zhang, K.A.I.; Lv, L.-P.; Wang, Y. Halogen-functionalized triazine-based organic frameworks towards high performance supercapacitors. *Chem. Eng. J.* **2020**, *400*, 125967. [CrossRef]

48. Zhang, F.; Wei, S.; Wei, W.; Zou, J.; Gu, G.; Wu, D.; Bi, S.; Zhang, F. Trimethyltriazine-derived olefin-linked covalent organic framework with ultralong nanofibers. *Sci. Bull.* **2020**, *65*, 1659–1666. [CrossRef]

49. Li, L.; Lu, F.; Guo, H.; Yang, W. A new two-dimensional covalent organic framework with intralayer hydrogen bonding as supercapacitor electrode material. *Micropor. Mesopor. Mat.* **2021**, *312*, 110766. [CrossRef]

50. Lin, K.Y.; El-Mahdy, A.F.M. Covalent triazine frameworks based on triphenylpyridine building block for high-performance supercapacitor and selective CO$_2$ capture. *Mater. Chem. Phys.* **2022**, *281*, 125850. [CrossRef]

51. Li, T.; Zhang, W.-D.; Liu, Y.; Li, Y.; Cheng, C.; Zhu, H.; Yan, X.; Li, Z.; Gu, Z.-G. A two-dimensional semiconducting covalent organic framework with nickel(ii) coordination for high capacitive performance. *J. Mater. Chem. A* **2019**, *7*, 19676–19681. [CrossRef]

52. Haldar, S.; Rase, D.; Shekhar, P.; Jain, C.; Vinod, C.P.; Zhang, E.; Shupletsov, L.; Kaskel, S.; Vaidhyanathan, R. Incorporating Conducting Polypyrrole into a Polyimide COF for Carbon-Free Ultra-High Energy Supercapacitor. *Adv. Energy Mater.* **2022**, *12*, 2200754. [CrossRef]

53. Wang, W.; Kale, V.S.; Cao, Z.; Kandambeth, S.; Zhang, W.; Ming, J.; Parvatkar, P.T.; Abou-Hamad, E.; Shekah, O.; Cavallo, L.; et al. Phenanthroline Covalent Organic Framework Electrodes for High-Performance Zinc-Ion Supercapattery. *ACS Energy Lett.* **2020**, *5*, 2256–2264. [CrossRef]

54. Kandambeth, S.; Jia, J.; Wu, H.; Kale, V.S.; Parvatkar, P.T.; Czaban-Jozwiak, J.; Zhou, S.; Xu, X.; Ameur, Z.O.; Abou-Hamad, E.; et al. Covalent Organic Frameworks as Negative Electrodes for High-Performance Asymmetric Supercapacitors. *Adv. Energy Mater.* **2020**, *10*, 2001673. [CrossRef]

55. Sajjad, M.; Tao, R.; Qiu, L. Phosphine based covalent organic framework as an advanced electrode material for electrochemical energy storage. *J. Mater. Sci. Mater. Electron.* **2021**, *32*, 1602–1615. [CrossRef]

56. Iqbal, R.; Badshah, A.; Ma, Y.-J.; Zhi, L.-J. An Electrochemically Stable 2D Covalent Organic Framework for High-performance Organic Supercapacitors. *Chin. J. Polym. Sci.* **2020**, *38*, 558–564. [CrossRef]

57. Yusran, Y.; Li, H.; Guan, X.; Li, D.; Tang, L.; Xue, M.; Zhuang, Z.; Yan, Y.; Valtchev, V.; Qiu, S.; et al. Exfoliated Mesoporous 2D Covalent Organic Frameworks for High-Rate Electrochemical Double-Layer Capacitors. *Adv. Mater.* **2020**, *32*, 1907289. [CrossRef]

58. El-Mahdy, A.F.M.; Zakaria, M.B.; Wang, H.-X.; Chen, T.; Yamauchi, Y.; Kuo, S.-W. Heteroporous bifluorenylidene-based covalent organic frameworks displaying exceptional dye adsorption behavior and high energy storage. *J. Mater. Chem. A* **2020**, *8*, 25148–25155. [CrossRef]

59. Li, C.; Yang, J.; Pachfule, P.; Li, S.; Ye, M.Y.; Schmidt, J.; Thomas, A. Ultralight covalent organic framework/graphene aerogels with hierarchical porosity. *Nat. Commun.* **2020**, *11*, 4712. [CrossRef]

60. Peng, C.; Yang, H.; Chen, S.; Wang, L. Supercapacitors based on three-dimensional porous carbon/covalent-organic framework/polyaniline array composites. *J. Energy Storage* **2020**, *32*, 101786. [CrossRef]

61. Xiong, S.; Liu, J.; Wang, Y.; Wang, X.; Chu, J.; Zhang, R.; Gong, M.; Wu, B. Solvothermal synthesis of triphenylamine-based covalent organic framework nanofibers with excellent cycle stability for supercapacitor electrodes. *J. Appl. Polym. Sci.* **2021**, *139*, 51510. [CrossRef]

62. Peng, H.; Huang, S.; Tranca, D.; Richard, F.; Baaziz, W.; Zhuang, X.; Samorì, P.; Ciesielski, A. Quantum Capacitance through Molecular Infiltration of 7,7,8,8-Tetracyanoquinodimethane in Metal–Organic Framework/Covalent Organic Framework Hybrids. *ACS Nano* **2021**, *15*, 18580–18589. [CrossRef] [PubMed]

63. Wu, Y.; Yan, D.; Zhang, Z.; Matsushita, M.M.; Awaga, K. Electron Highways into Nanochannels of Covalent Organic Frameworks for High Electrical Conductivity and Energy Storage. *ACS Appl. Mater. Interfaces* **2019**, *11*, 7661–7665. [CrossRef]

64. Mohammed, A.K.; Vijayakumar, V.; Halder, A.; Ghosh, M.; Addicoat, M.; Bansode, U.; Kurungot, S.; Banerjee, R. Weak Intermolecular Interactions in Covalent Organic Framework-Carbon Nanofiber Based Crystalline yet Flexible Devices. *ACS Appl. Mater. Interfaces* **2019**, *11*, 30828–30837. [CrossRef]

65. Xu, Z.; Liu, Y.; Wu, Z.; Wang, R.; Wang, Q.; Li, T.; Zhang, J.; Cheng, J.; Yang, Z.; Chen, S.; et al. Construction of extensible and flexible supercapacitors from covalent organic framework composite membrane electrode. *Chem. Eng. J.* **2020**, *387*, 124071. [CrossRef]

66. Zhao, X.; Sajjad, M.; Zheng, Y.; Zhao, M.; Li, Z.; Wu, Z.; Kang, K.; Qiu, L. Covalent organic framework templated ordered nanoporous C60 as stable energy efficient supercapacitor electrode material. *Carbon* **2021**, *182*, 144–154. [CrossRef]

67. Patra, B.C.; Bhattacharya, S. New Covalent Organic Square Lattice Based on Porphyrin and Tetraphenyl Ethylene Building Blocks toward High-Performance Supercapacitive Energy Storage. *Chem. Mater.* **2021**, *33*, 8512–8523. [CrossRef]

68. Haldar, S.; Kushwaha, R.; Maity, R.; Vaidhyanathan, R. Pyridine-Rich Covalent Organic Frameworks as High-Performance Solid-State Supercapacitors. *ACS Mater. Lett.* **2019**, *1*, 490–497. [CrossRef]

69. Halder, A.; Ghosh, M.; Khayum, M.A.; Bera, S.; Addicoat, M.; Sasmal, H.S.; Karak, S.; Kurungot, S.; Banerjee, R. Interlayer Hydrogen-Bonded Covalent Organic Frameworks as High-Performance Supercapacitors. *J. Am. Chem. Soc.* **2018**, *140*, 10941–10945. [CrossRef]

70. Kushwaha, R.; Haldar, S.; Shekhar, P.; Krishnan, A.; Saha, J.; Hui, P.; Vinod, C.P.; Subramaniam, C.; Vaidhyanathan, R. Exceptional Capacitance Enhancement of a Non-Conducting COF through Potential-Driven Chemical Modulation by Redox Electrolyte. *Adv. Energy Mater.* **2021**, *11*, 2003626. [CrossRef]